International Journal of Scientific Engineering and Research (IJSER)
ISSN (Online): 2347-3878
Index Copernicus Value (2015): 56.67 | Impact Factor (2017): 5.156

B3LYP-D3/6-311G (d,p) Level of Theory to Explain Corrosion Inhibitive Properties of Five Cationic Gemini Surfactant from Series 14-n-14 and 16-n-16

Sheerin Masroor[1], M. Mobin[2], Anil Kumar Singh[3], M. J. Alam[4], Shabbir Ahmad[5]

[1, 3]Department of Chemistry, Anugrah Narayan College, Patliputra University, Patna, 800013

[2]Department of Applied Chemistry, Faculty of Engineering and Technology, Aligarh Muslim University, Aligarh (U.P) 202002-India

[4, 5]Department of Physics, Faculty of Science, Aligarh Muslim University, Aligarh (U.P) 202002-India

Abstract: ***Paper presents a comparative study of five synthesized cationic Gemini surfactants belonging to two series of tetradecyl (14-n-14) and hexadecyl (16-n-16) with methyl spacers, such as butane diyl-1,4-bis(dimethyl tetradecyl ammonium bromide), hexane diyl-1,6-bis(dimethyl tetradecyl ammonium bromide), butane diyl-1,4-bis(dimethyl hexadecyl ammonium bromide), pentane diyl-1,5-bis(dimethyl hexadecyl ammonium bromide), hexane diyl-1,6-bis(dimethyl hexadecyl ammonium bromide) as corrosion obstacle for acidic corrosion of mild steel via theoretical chemical calculations. The Quantum chemical calculations have been carried out at B3LYP-D3/6-311G(d,p) level of theory to obtain some structure based parameters that are relevant to corrosion inhibition efficiency as well as to supplement the experimental data for the present compounds. An empirical dispersion correction to hybrid functional (B3LYP-D3) has been incorporated in the present calculations due to presence of non-covalent interactions, Br……H, in the present compounds.***

Keywords: B3LYP-D3/6-311G(d,p), Quantum chemical calculations, Cationic Gemini Surfactant

1. Introduction

Corrosion is the most problematic phenomenon so far as concerned for metals. Metals destroy their existence via this means. Earlier various techniques were applied to measure the percent suppress or inhibition of corrosion by different inhibitors. Some of the experimental techniques involved are gravimetric analysis, potentiodynamic polarization techniques, electrochemical impedance spectroscopy, metal ion analysis of solution and UV-Visible spectroscopy. The need of hour is the application of technique that saves time and money to be invested. As experimental techniques needs a lot of time and chemicals to be consume to get result. As indicated from previous literature, it is observed that the compounds having hetero atoms i.e., consisting of a π-system and/or N, O, S gives good corrosion inhibition comparable to other organic compounds [1-5]. Among various compounds containing N or Br, as corrosion inhibitors, Gemini surfactants are considered to be excellent class of inhibitors to suppress corrosion. [6-7]. These ammonium based compounds are not only used for steel as inhibitor but also for aluminium, zinc [8-9]. Quantum mechanical methods like density functional theory (DFT) have become powerful tool to explain the mechanism of corrosion inhibition with the help of structure based molecular parameters such as reactivity descriptors, dipole moment, atomic charges and molecular electrostatic potential. The reactivity of the corrosion inhibitors are explained by some reactivity descriptors based on frontier molecular orbitals (HOMO and LUMO) energies as the reactivity is closely related to the highest occupied molecular orbital (HOMO) and lowest unoccupied molecular orbital (LUMO) energy Eigen values. The hybrid functional B3LYP (Becke, 3-parameter, Lee-Yang-Parr) have been applied widely to compute the molecular parameters related to the inhibition action [10, 11]. In this work, the inhibition action of the compounds 14-4-14, 14-6-14, 16-4-16, 16-5-16 and 16-6-16 on corrosion has been studied with the help of various theoretical molecular parameters obtain at B3LYP-D3/6-311G(d,p) level of theory.

1.1 Experimental details

The experimental analysis includes gravimetric measurements, solution analysis of metal ions, potentiodynamic polarization analysis and electrochemical impedance spectroscopy [12, 13].

1.2 Theoretical/Computational details

The DFT calculations implemented in Gaussian 09 [14] software were performed on compounds14-4-14, 14-6-14, 16-4-16, 16-5-16 and 16-6-16 in their ground electronic states. The dispersion corrected hybrid functional B3LYP-D3 [15] along with triple zeta basis set 6-311G(d,p) was employed to compute molecular structure, IR spectra and various other molecular parameters in the vacuo. The Grimme's D3 correction in B3LYP was used due to presence of Br…H-C interactions in molecule. Pure Lorentzian band shape with FWHM of 6 cm^{-1} was used to plot the simulated IR spectra of the present molecules. The visualization program GaussView 5 was used to generate molecular structure sketches with numbering scheme, HOMO, LUMO plots and molecular electrostatic potential map (MEP) diagrams for the present molecules. All compounds were

optimized in their ground electronic states under tight convergence criterion. In all cases, the optimized structures of compounds were found on minimum on the potential energy surface as it confirmed by calculating the corresponding real IR frequencies at the same level of theory. In geometry optimization calculations, molecular parameters like minimum self-consistent field (SCF) energy, dipole moment, atomic charges, HOMO and LUMO energy Eigen values have been obtained. The equations reported elsewhere [16-18] were used to compute chemical reactivity descriptors based on HOMO-LUMO orbital energies.

2. Result and Discussion

2.1 Comparative Experimental Details

The synthesized cationic Gemini surfactants from series 14-n-14 and 16-n-16, were served as corrosion inhibitors for different media. As obtained corrosion inhibition efficiencies comparatively obtained are in the order: [12, 13].

For 16-n-16 series:
16-5-16 < 16-6-16 < 16-4-16 in formic acid media.
And for 14-n-14 series
14-6-14 < 14-4-14 in 1 M HCl media.

2.2 Theoretical Details

The optimized molecular geometry of the 14-4-14, 14-6-14, 16-4-16, 16-5-16 and 16-6-16 are shown with numbering scheme along with the direction of dipole moment vector in Fig 1 and 2. Theoretical IR spectra obtained at optimized geometry have been compared with FTIR and they are found in good agreement. The comparisons of simulated and experimental IR spectra have been depicted along with important band assignments in Fig. 1S-5S (Supplementary materials). The IR band assignments have been made by visualization of atomic displacements GaussView 5 software [19]. The bands due to C-H stretching and in-plane bending vibrations have been observed around 3000 cm^{-1} and 1450 cm^{-1} respectively in the present FTIR spectra. Some C-H vibrations have been shifted towards the lower wavenumber due to presence of non-covalent interactions, H…Br. It is necessary to obtain accurate structure and orientation of the molecules for better understanding of their corrosion inhibition performance. Quantum chemical parameters such as reactivity descriptors obtained using molecular orbital energies, dipole moment, electrostatic potential mapped on to electron density, total energy, atomic charges, HOMO-LUMO energies and gap between them correlate with the corrosion protection efficiency of organic inhibitors [20-24]. Molecular energy, dipole moment, HOMO-LUMO energies, HOMO-LUMO gap and global chemical reactivity descriptors are depicted in Table 1.

The atomic charges and dipole moment of the molecules play important role to define electrostatic interactions between molecules and metal surface during physical adsorption. The Mulliken's atomic charges have been computed for the present molecules as they are responsible for electrostatic interactions. The comparisons of Mulliken's atomic charges of 14-4-14, 14-6-14, 16-4-16, 16-5-16 and 16-6-16 are shown in Fig 3 and 4. The more negative charge on active atoms defines the more electron density over there and therefore there will be the stronger binding capability with metal surface. From the Fig 3, the atoms 1C, 18N, 25N, 41C, 117Br and 118Br in 14-4-14 and 14-6-14 molecule have large negative charges. In Fig 4, the charges on atoms 17N, 24N, 115Br, 116Br, 117C, 118C, 124C and 125C in 16-4-16, 16-5-16 and 16-6-16 molecules are predicted with large negative values. These atoms with high negative values in present molecules may show stronger binding capability with metal surface. The charge on Br atom follows this order 14-6-14 > 16-6-16 > 16-4-16 > 14-4-14 > 16-4-16. Dipole moment is another important physical quantity that defines polarity of molecule. In present molecules, the large dipole moment values have been predicted for 14-5-14 and 16-6-16 molecules. No significant correlation between the dipole moment and inhibition efficiency has been found in the literature [25, 26].

The chemical activity of the corrosion inhibitors is closely related to the frontier molecular orbitals (HOMO and LUMO). During adsorption, one of the chemical species acts as electrons donor and another acts as electrons acceptor. Thus, adsorption of molecule on to metal surface can be defined as the interaction between HOMO and LUMO of two reacting chemical species. These molecular orbitals are used to predict the active centers of adsorption for the inhibitor molecules. The spatial diagrams of HOMO and LUMO of the present compounds are shown in Fig 5 and 6. In these diagrams, the HOMO's are extended mainly over the Br atoms while the LUMO's are located over the middle part of the long chain compounds. These diagrams show the charge transfer properties from Br atoms to middle part of the compounds. Therefore, these information's confirm that middle part of the present compounds has participated in chemical reaction during adsorption. The energy Eigen values of HOMO and LUMO define the ability to donate and accept the electron respectively while the energy gap between HOMO and LUMO describe the strength of the interaction between two reacting species. The low value of gap ascribe to compound as more reactivate. The increasing energy Eigen value of HOMO of the compounds makes easy the adsorption process by donating electrons to acceptor metal and therefore enhances the inhibition efficiency [27-29]. Similarly, low value of HOMO-LUMO gap shows high inhibition efficiency [30-32]. In this study, the high value of HOMO and low value of HOMO-LUMO gap are predicted for the compound 14-6-14 which indicates its better inhibitor efficiency. The global reactivity descriptors based on HOMO and LUMO energy Eigen values of the present compounds are presented in Table 1. The calculated reactivity descriptors such as ionization potential, electron affinity, chemical hardness, softness, chemical potential, electrophilicity, back-donation energy and fraction of electron transferred during adsorption are the important quantities that define the corrosion inhibitor efficiency of the compounds. The value of fraction of electron transferred (ΔN) is found larger for the 14-6-14 molecule among others which is considered to be good inhibitor. As per Lukovit's study if $\Delta N < 3.6$, the inhibition efficiency of inhibitors enhances to donate electrons to the metal surface [33]. The back-donation energy values which governing the interaction between the inhibitor and metal surface are

estimated for the present compounds as given in Table 1 [34]. The absolute electrophilicity index measures the ability of molecule to accept electrons. In this work, its high value is estimated for 14-6-14.

Moreover, the molecular electrostatic potential (MEP) mapping on to electron density for the present molecules has been presented in Fig. 7 and 8. The most negative and positive electrostatic potentials are assigned to red and blue colour respectively while the neutral regions are assigned to green colour. The negative potential surfaces in MEP can be considered as nucleophilic centres, whereas regions with positive potential are electrophilic sites. In the present case, the regions over the Br atoms may be considered as nucleophilic sites whereas surfaces over the N atoms may be regarded as electrophilic centres. The carbon chains with hydrogen atoms shown by green colour are the neutral.

3. Conclusion

After doing experimental chemical calculations the corrosion inhibition property of the synthesized compounds were further proved by Quantum chemical calculations. It was found that the five synthesized cationic Gemini surfactants such as butane diyl-1,4-bis(dimethyl tetradecyl ammonium bromide), hexane diyl-1,6-bis(dimethyl tetradecyl ammonium bromide), butane diyl-1,4-bis(dimethyl hexadecyl ammonium bromide), pentane diyl-1,5-bis(dimethyl hexadecyl ammonium bromide), hexane diyl-1,6-bis(dimethyl hexadecyl ammonium bromide), have inhibition efficiencies in the given order from the various chemical descriptors obtained using HOMO and LUMO energy eigen values suggest the following order of good inhibitors:

a) Dipole moment: 14-6-14 > 16-6-16 > 14-4-14 > 16-4-16 > 16-5-16
b) HOMO-LUMO gap: 14-6-14 > 16-6-16 > 16-4-16 > 16-5-16 > 14-4-14
c) ΔN: 14-6-14 > 16-6-16 > 16-4-16 > 16-5-16 > 14-4-14
d) Electrophilicity: 14-6-14 > 16-6-16 > 16-5-16 > 16-4-16 > 14-4-16

Thus the compound 14-6-14 and 16-6-16 can be considered as good inhibitors among others on the basis of chemical descriptors.

4. Conflict of Interest

There is no conflict of interest on behalf of all the authors.

References

[1] Khaled K F (2003) The inhibition of benzimidazole derivatives on corrosion of iron in 1 M HCl solutions, Electrochim. Acta 48:2493–2503.
[2] Bentiss F, Lagrenee M, Traisnel M, Hornez JC (1999) The corrosion inhibition of mild steel in acidic media by a new triazole derivative, Corros. Sci. 41:789–803.
[3] Gece G (2011) Drugs: A review of promising novel corrosion inhibitors, Corros. Sci. 53:3873–3898.
[4] Moretti G, Guidi F, Fabris F (2013) Corrosion inhibition of the mild steel in 0.5 M HCl by 2-butyl-hexahydropyrrolo[1,2-b][1,2]oxazole, Corros. Sci. 76:206–218.
[5] Ayyannan G, Karthikeyan K, Vivekananthan S S, Gopiraman M, Rathinavelu A (2013) Chemical and electrochemical investigations of high carbon steel corrosion inhibition in 10 % HCl medium by quinoline chalcones, Ionics 19:919–932.
[6] Achouri M El, Kertit S, Gouttaya H M, Nciri B, Bensouda Y, Perez L, Infante M R, Elkacem K (2001) Corrosion inhibition of iron in 1 M HCl by some gemini surfactants in the series of alkanediyl-α,ω-bis-(dimethyl tetradecyl ammonium bromide), Prog. Org. Coat., 43:267–273.
[7] Ling-Guang Qiu, , An-Jian Xie, Yu-Hua Shen (2005) The adsorption and corrosion inhibition of some cationic gemini surfactants on carbon steel surface in hydrochloric acid, Corros. Sci, 47:273–278.
[8] Huang W, Zhao J (2006) Adsorption of quaternary ammonium gemini surfactants on zinc and the inhibitive effect on zinc corrosion in vitriolic solution, Colloids and Surfaces A: Physicochemical and Engineering Aspects, 278 :246–251.
[9] Zhang Q, Z. Gao, , F. Xu, X. Zou, Adsorption and corrosion inhibitive properties of gemini surfactants in the series of hexanediyl-1,6-bis-(diethyl alkyl ammonium bromide) on aluminium in hydrochloric acid solution, Colloids and Surfaces A: Physicochemical and Engineering Aspects, 380 (2011) 191–200.
[10] Becke AD (1993) Density-functional thermochemistry. III. The role of exact exchange J. Chem. Phys. 98:5648-5652.
[11] Lee C, Yang W, Parr RG (1988) Development of the Colle-Salvetti correlation-energy formula into a functional of the electron density, Phys. Rev. B, 37:785-789
[12] Mobin M, Masroor S (2012) Alkanediyl-α, ω-bis (Dimethyl Cetylammonium Bromide) Gemini Surfactants as Novel Corrosion Inhibitors for Mild Steel in Formic Acid, Mater. Research. 15:837-847.
[13] Mobin M, Masroor S (2012) Cationic Gemini Surfactants as Novel Corrosion Inhibitor for Mild Steel in 1M HCl, Int. J. Electrochem. Sci., 7:6920 – 6940.
[14] M.J. Frisch, et al., Gaussian 09, Revision D.01, Gaussian Inc, Wallingford CT, 2009.
[15] Grimme S, Antony J, Ehrlich S, Krieg H (2010) A consistent and accurate ab initio parametrization of density functional dispersion correction (DFT-D) for the 94 elements H-Pu, J. Chem. Phys. 132:154104.
[16] Pearson R G (1990) Hard and soft acids and bases—the evolution of a chemical concept, Coordination Chemistry Reviews, 100:403-425
[17] Rajendran, M.; Malkiya, A.; Muthupetchi, P.; Devapiriam, D (2016) DFT approach on corrosion inhibition performance on thiosemicarbazone derivatives on metallic iron. Journal of Advanced Scientific Research. 7(1): 32-37.
[18] Dandia A, Gupta S L, Sudheer A, Quraishi (2012) Microwave Assisted Economic Synthesis of 4-amino-3-alkyl-5-mercapto-1, 2, 4-triazole Derivatives as Green Corrosion Inhibitors for Copper in Hydrochloric Acid M A, J. Mater. Environ. Sci., 3:993-1000.
[19] R. Dennington, T. Keith, J. Millam, GaussView, Ver. 5, Semichem Inc., Shawnee Mission KS, 2009.

[20] Mistry B M, Patels N S, Jauhari S (2012) Experimental and quantum chemical studies on corrosion inhibition performance of quinoline derivatives for MS in 1N HCl, et al Bull. Mater. Sci., 35:459–469.
[21] Patel N S, Jauhari S, Mehta G N (20100 The Inhibition of Mild Steel Corrosion in 1 N HCl by Imidazole Derivatives, Acta Chim. Slov. 57:297-304
[22] Bahrami M.J, Hosseini S M A, Pilvar P (2010) Experimental and theoretical investigation of organic compounds as inhibitors for mild steel corrosion in sulfuric acid medium, 2010 Corros. Sci. 52:2793-2803.
[23] Gece G, Bilgic S (2010) A theoretical study on the inhibition efficiencies of some amino acids as corrosion inhibitors of nickel, Corros. Sci. 52:3435-3443.
[24] Ayatia N S, Khandandela S, Momenia M, Moayeda M H, Davoodi A, Rahimizadeh M (2011) Experimental and quantum chemical studies on corrosion inhibition performance of quinoline derivatives for MS in 1N HCl, Mater. Chem. Phys. 126:873-879.
[25] Gao G, Liang C (2007) Electrochemical and DFT studies of β-amino-alcohols as corrosion inhibitors for brass, Electrochim. Acta 52:4554-4559.
[26] Khalil N (2003) Quantum chemical approach of corrosion inhibition, Electrochim. Acta 48 :2635-2640.
[27] Gece G, Bilgiç S (2010) A theoretical study of some hydroxamic acids as corrosion inhibitors for carbon steel, Corros. Sci. 52:3304–3308.
[28] Li S L, Wang Y G, Chen S H, Yu R, Lei S B, Ma H Y, Liu D X (1999) Some aspects of quantum chemical calculations for the study of Schiff base corrosion inhibitors on copper in NaCl solutions, Corros. Sci. 41:1769–1782.
[29] Fu J J, Li S N, Cao L H, Wang Y, Yan L H, Lu L D (2010) l-Tryptophan as green corrosion inhibitor for low carbon steel in hydrochloric acid solution, J. Mater. Sci. 45: 979– 986.
[30] Gece G, Bilgiç S, Gece G, S. Bilgiç / Corrosion Science 52 (2010) 3304–3308,
[31] Ozcan M, Dehri I, Erbil M (2004) Organic sulphur-containing compounds as corrosion inhibitors for mild steel in acidic media: correlation between inhibition efficiency and chemical structure, Appl. Surf. Sci. 236:155–164.
[32] Gece G, Bilgic S, Turksen O (2010) Quantum chemical studies of some amino acids on the corrosion of cobalt in sulfuric acid solution, Mater. Corros. 61:141–146.
[33] Lukovits I, Kalman E, Zucchi F (2001) Corrosion Inhibitors—Correlation between Electronic Structure and Efficiency, Corrosion. 57:3-7.
[34] Gomez B, Likhanova NV, Dominguez-Aguilar MA, Martinez-Palou R, Vela R, Gasquez J (2006) Quantum Chemical Study of the Inhibitive Properties of 2-Pyridyl-Azoles, J.Phy.Chem B, 110: 8928-8934.

Table

Table 1: Some structure based quantum chemical parameters for the different compounds as obtained at B3LYP-D3/6-311G (d,p) level of theory in the vacuo.

Parameters	14-4-14	14-6-14	16-4-16	16-5-16	16-6-16
SCF Energy (a.u.)	-6677.20655417	-6755.83442332	-6834.51461237	-6873.86424445	-6913.16064165
E_{HOMO} (eV)	-5.08	-3.95	-5.04	-5.13	-4.27
E_{LUMO} (eV)	0.23	-0.67	0.17	0.13	-0.56
Gap (eV)	5.31	3.28	5.21	5.26	3.71
Dipole Moment (Debye)	7.0211	31.1696	6.6412	5.4745	20.4949
Electronegativity	2.42	2.31	2.44	2.50	2.41
Chemical Hardness	2.66	1.64	2.61	2.63	1.86
Chemical Softness	0.19	0.31	0.19	0.19	0.27
Fraction of electron transferred, ΔN	0.86	1.43	0.87	0.86	1.23
Ionization potential	5.08	3.95	5.04	5.13	4.27
Electron affinity	0.23	0.67	0.17	0.13	0.56
Chemical potential	-2.42	-2.31	-2.44	-2.50	-2.41
Electrophilicity	1.10	1.63	1.14	1.19	1.56
Back-donation energy	-0.67	-0.41	-0.65	-0.66	-0.47

Figures

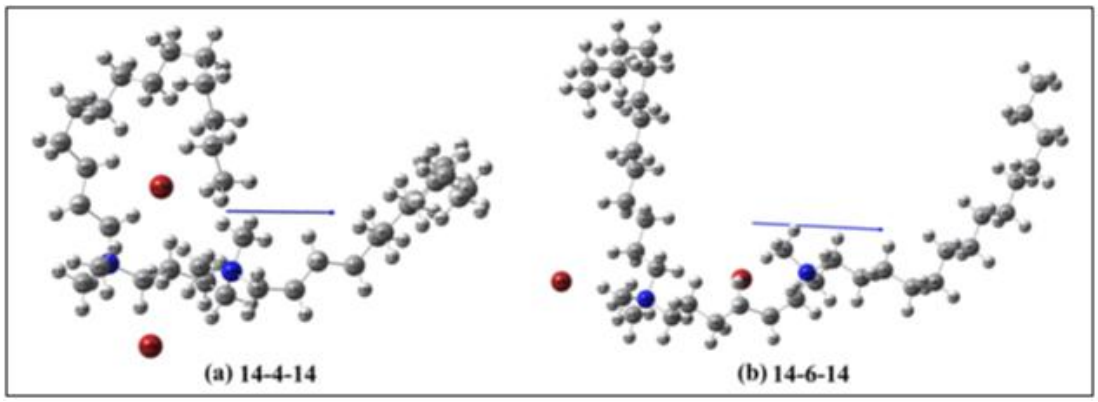

Figure 1: The optimized molecular geometry of the compounds (a) 14-4-14 and (b) 14-6-14

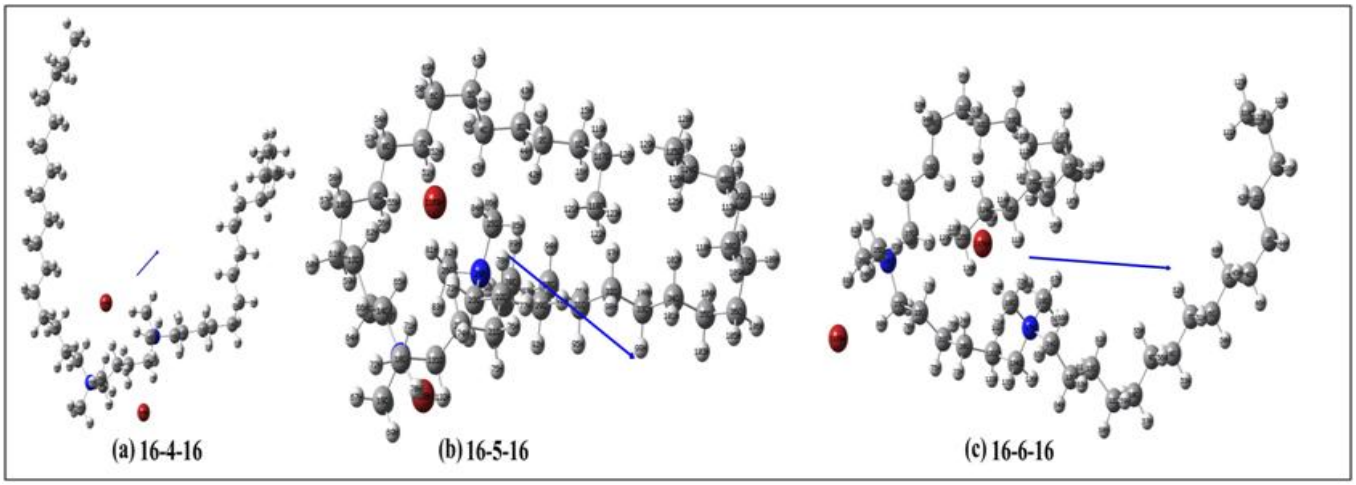

Figure 2: The optimized molecular geometry of the compounds (a) 16-4-16, (b) 16-5-16 and (c) 16-6-16.

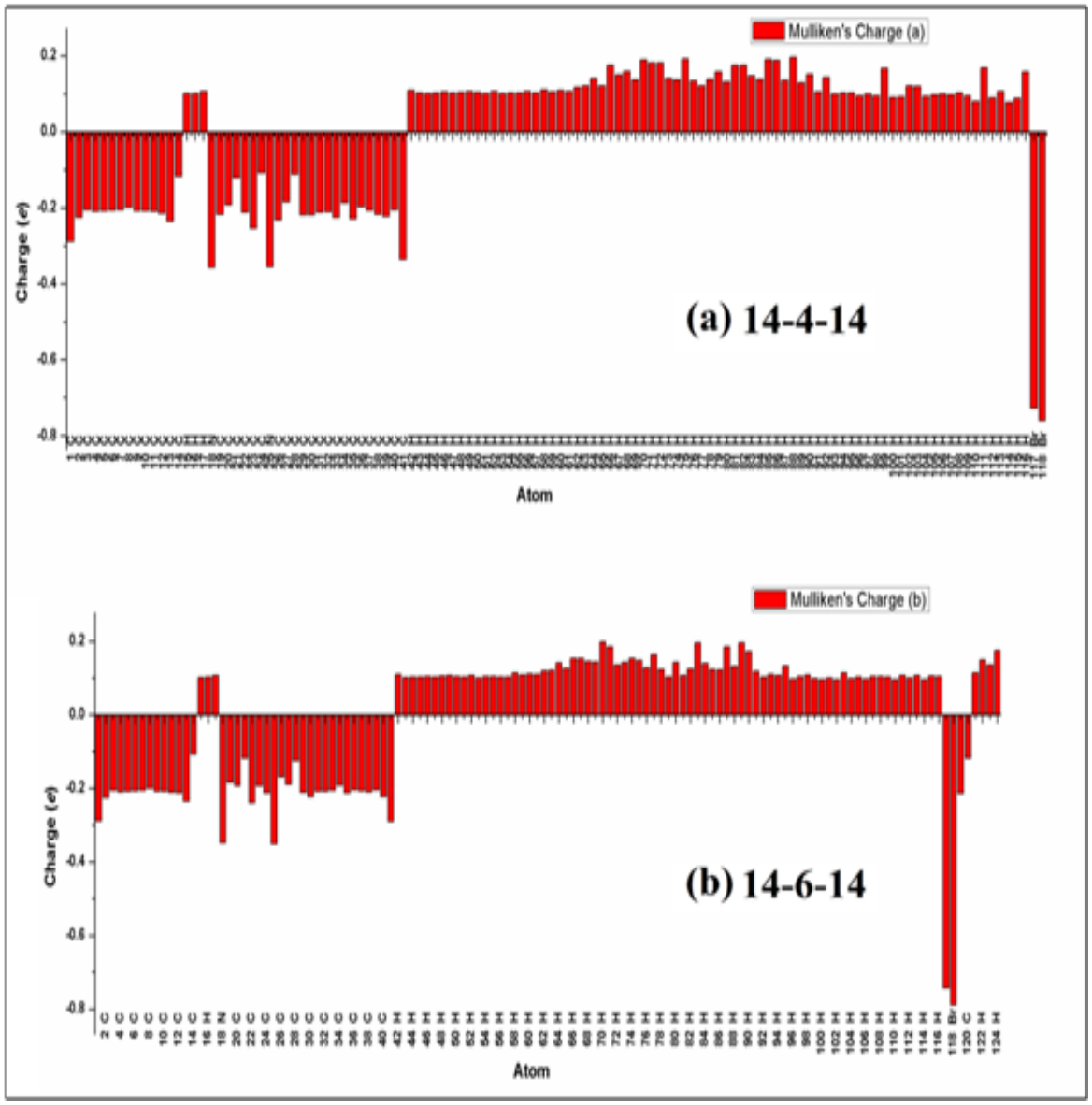

Figure 3: Comparisons of Mulliken's atomic charges in between compounds (a) 14-4-14 and (b) 14-6-14

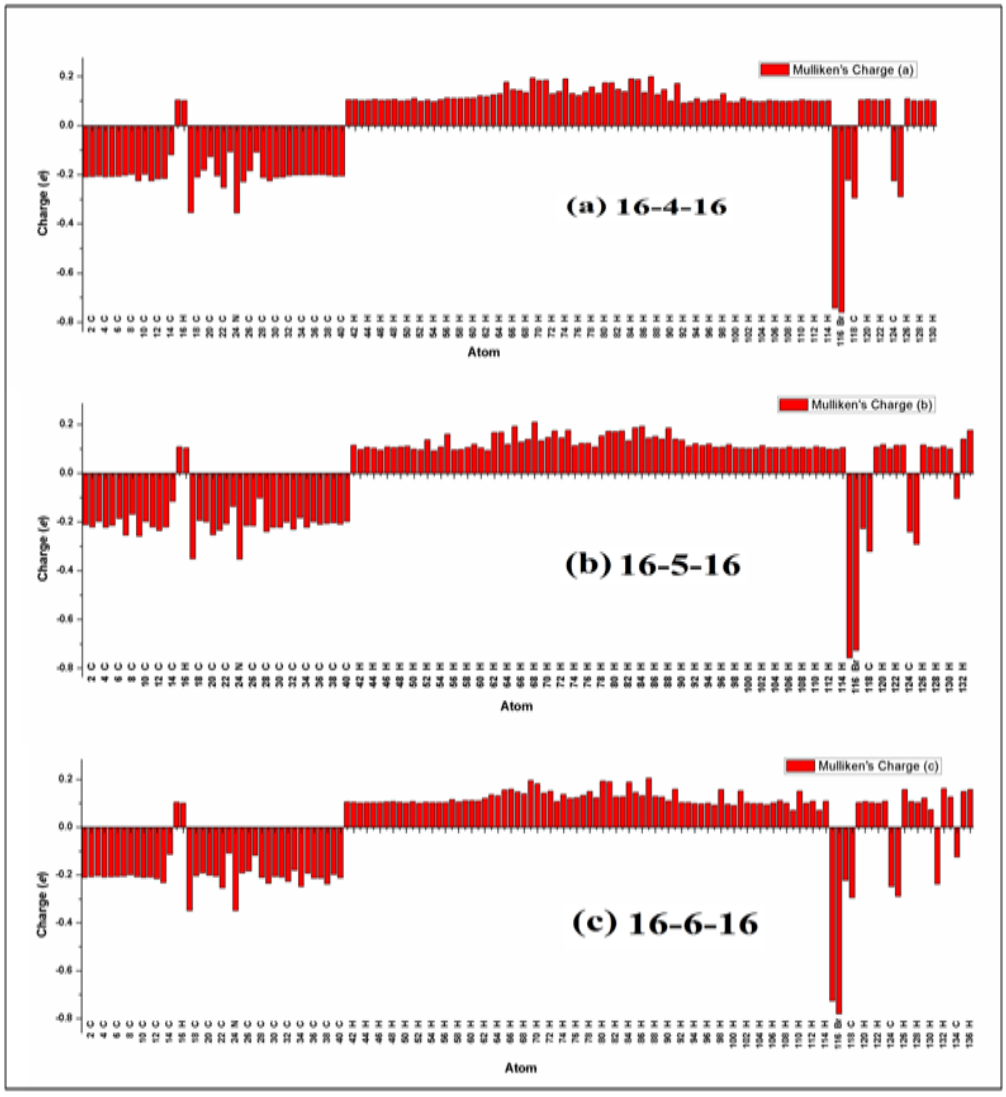

Figure 4: Comparisons of Mulliken's atomic charges in between (a) 16-4-16, (b) 16-5-16 and (c)16-6-16

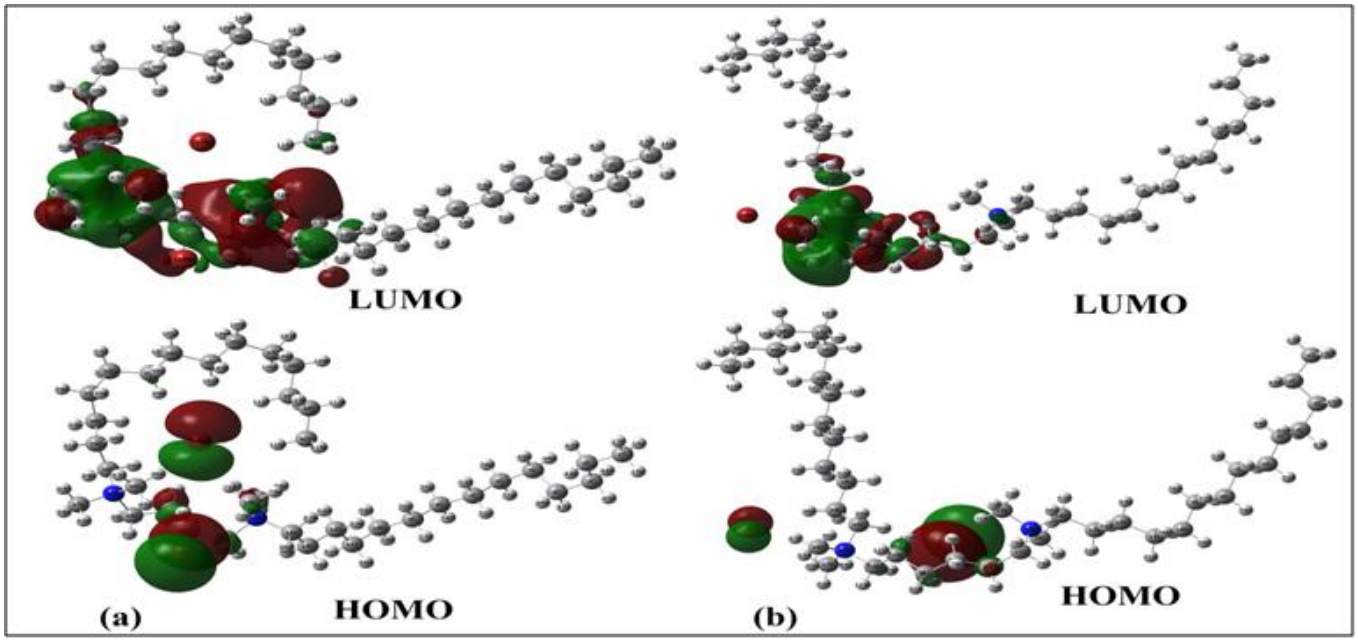

Figure 5: Spatial diagrams of HOMO and LUMO of compounds (a) 14-4-14 and (b) 14-6-14

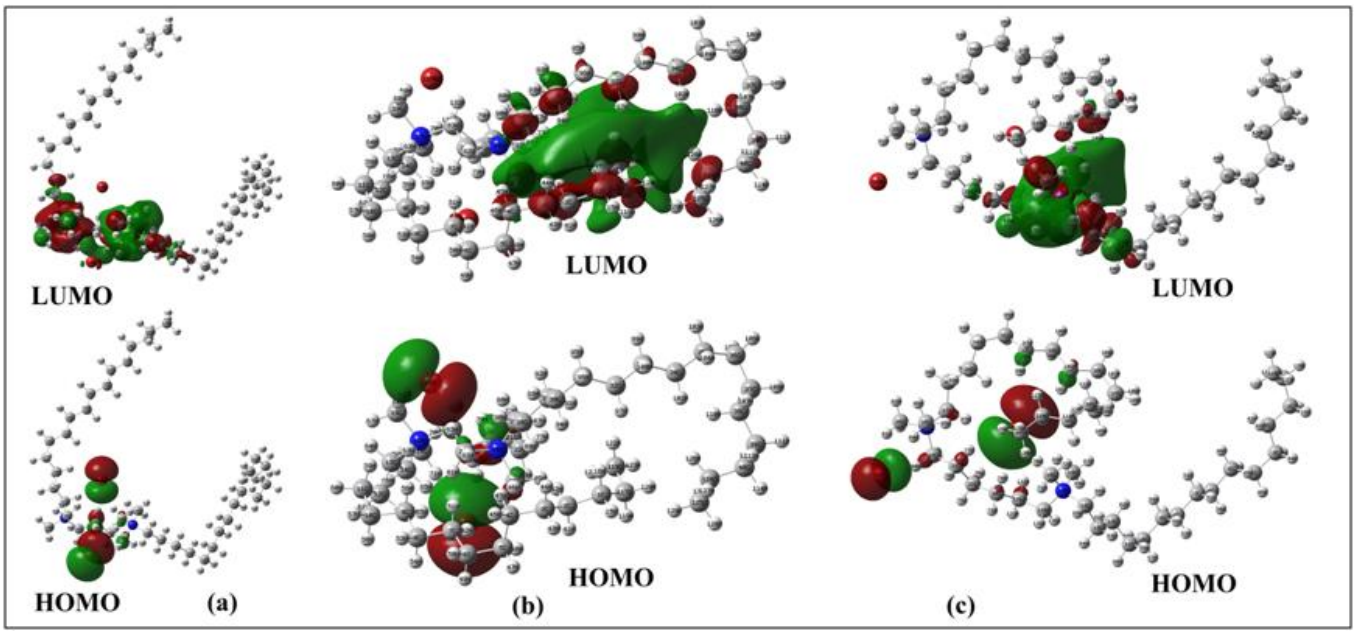

Figure 6: Spatial diagrams of HOMO and LUMO of compounds (a) 16-4-16, (b) 16-5-16 and (c) 16-6-16.

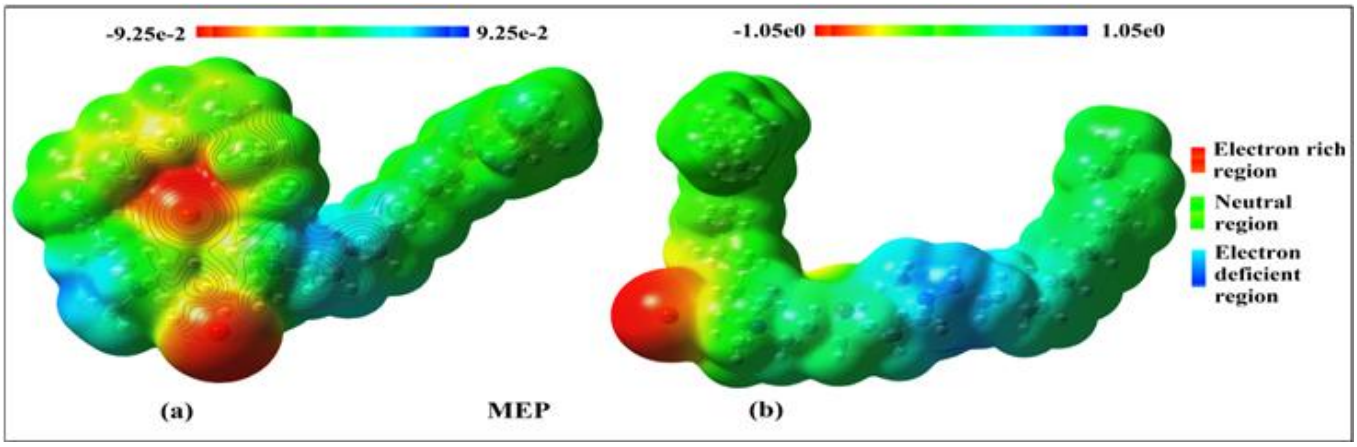

Figure 7: Molecular electrostatic potential (MEP) mapping on to electron density for compounds (a) 14-4-14 and (b) 14-6-14

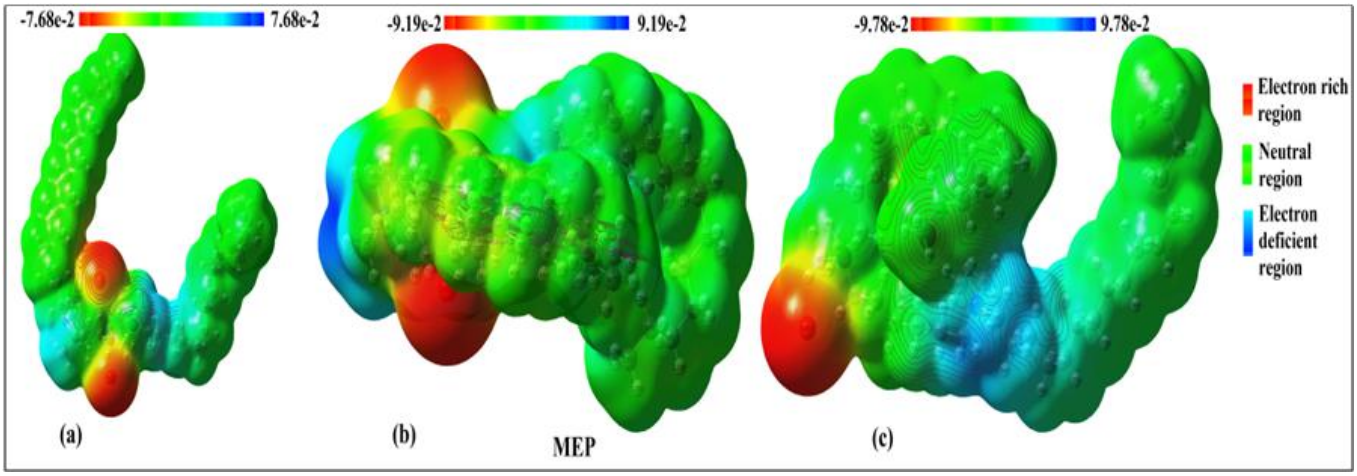

Figure 8: Molecular electrostatic potential (MEP) mapping on to electron density for compounds (a) 16-4-16, (b) 16-5-16 and (c) 16-6-16.

Supplementary Figures 1S-5S

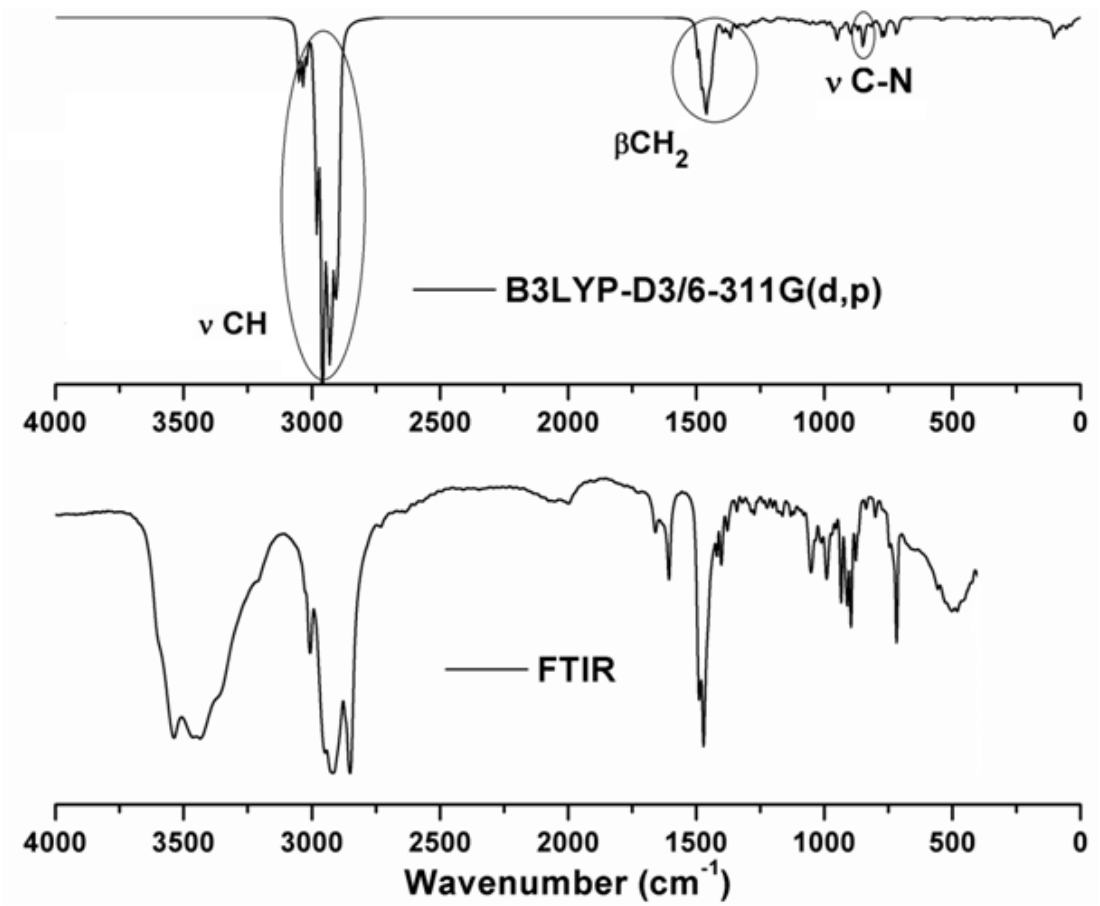

Figure 1S: Comparison of experimental and simulated IR spectra of 14-4-14 [ν: stretching, β: in-plane bending vibrations]

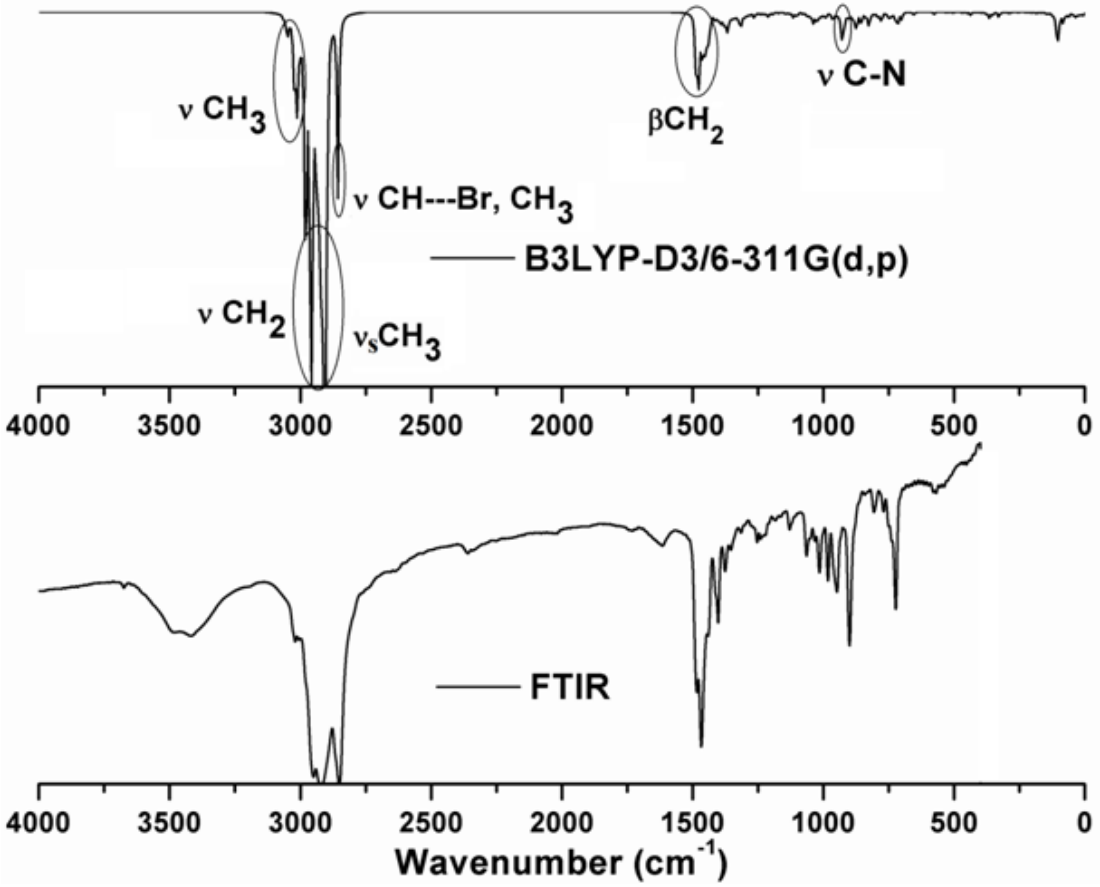

Figure 2S: Comparison of experimental and simulated IR spectra of 14-6-14 [ν: stretching, β: in-plane bending vibrations]

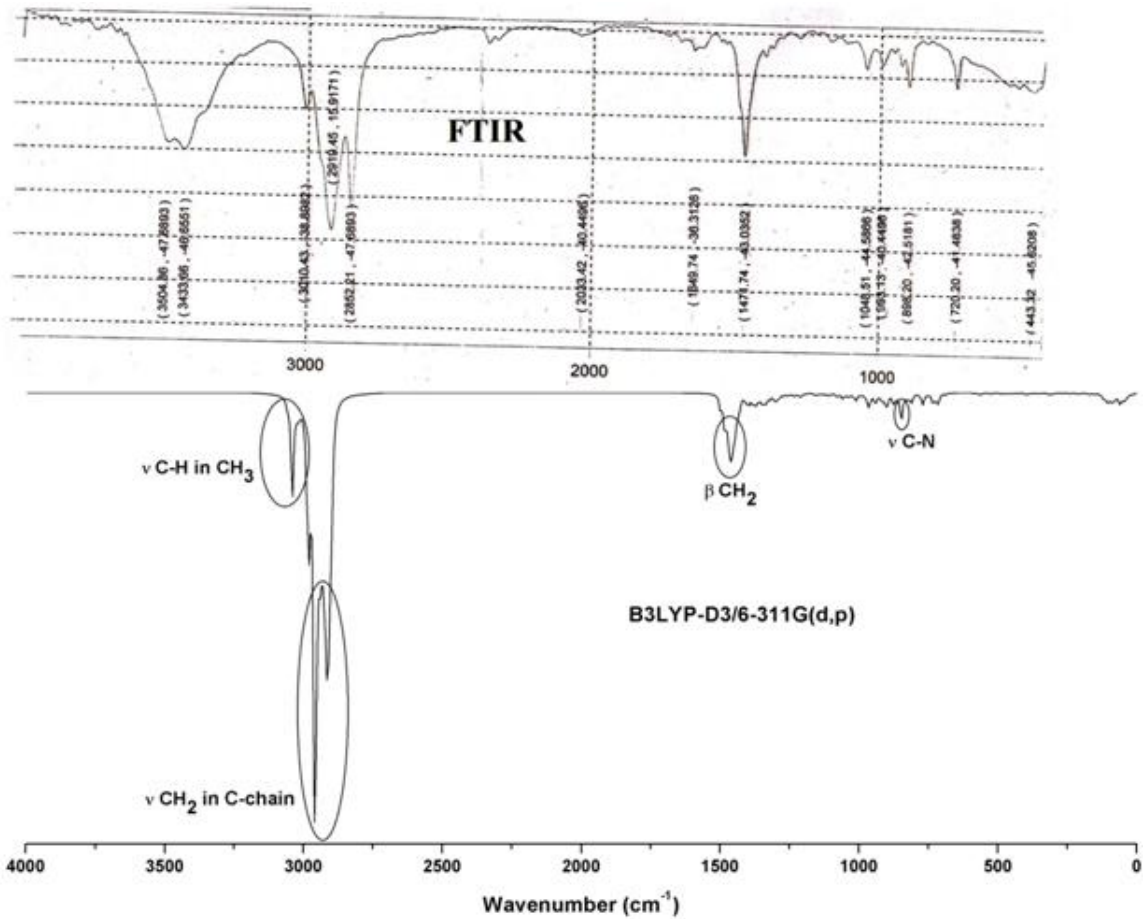

Figure 3S: Comparison of experimental and simulated IR spectra of 16-4-16 [ν: stretching, β: in-plane bending vibrations]

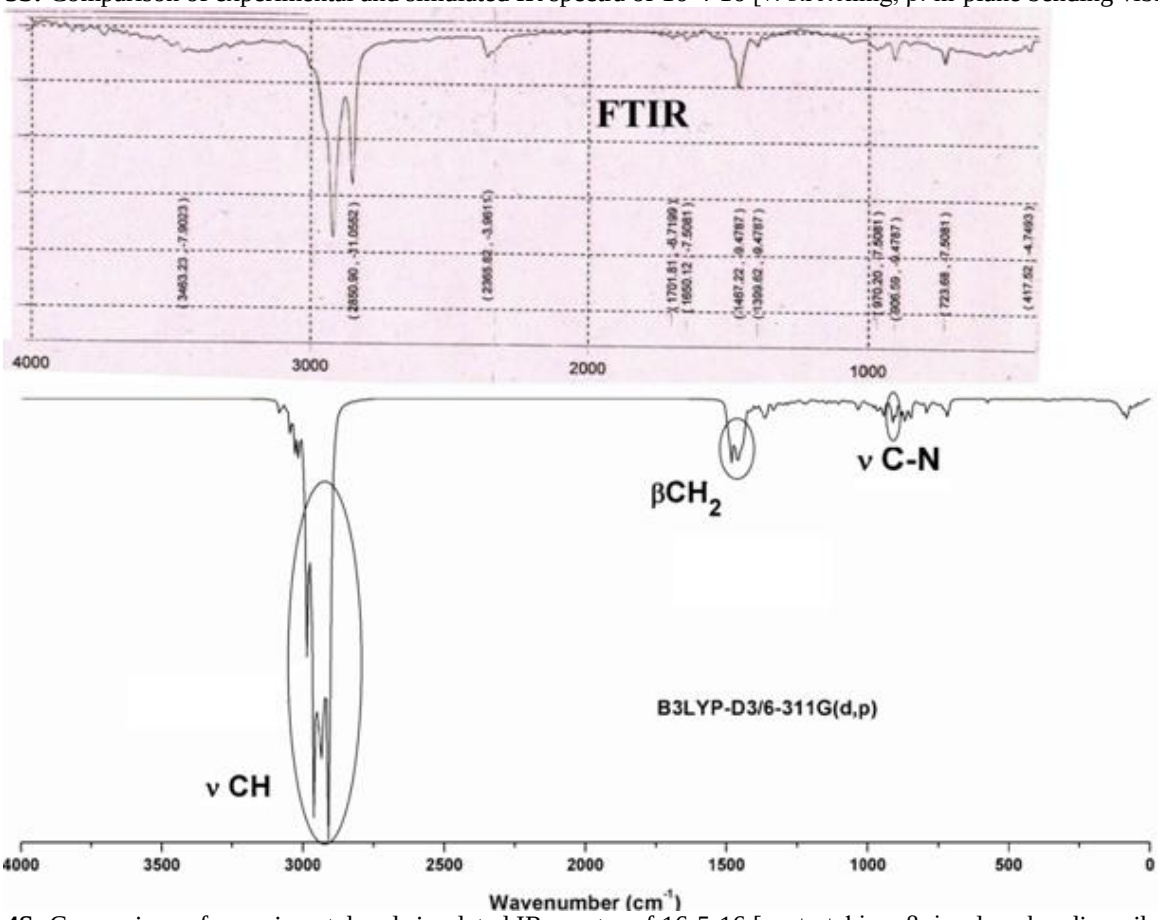

Figure 4S: Comparison of experimental and simulated IR spectra of 16-5-16 [ν: stretching, β: in-plane bending vibrations]

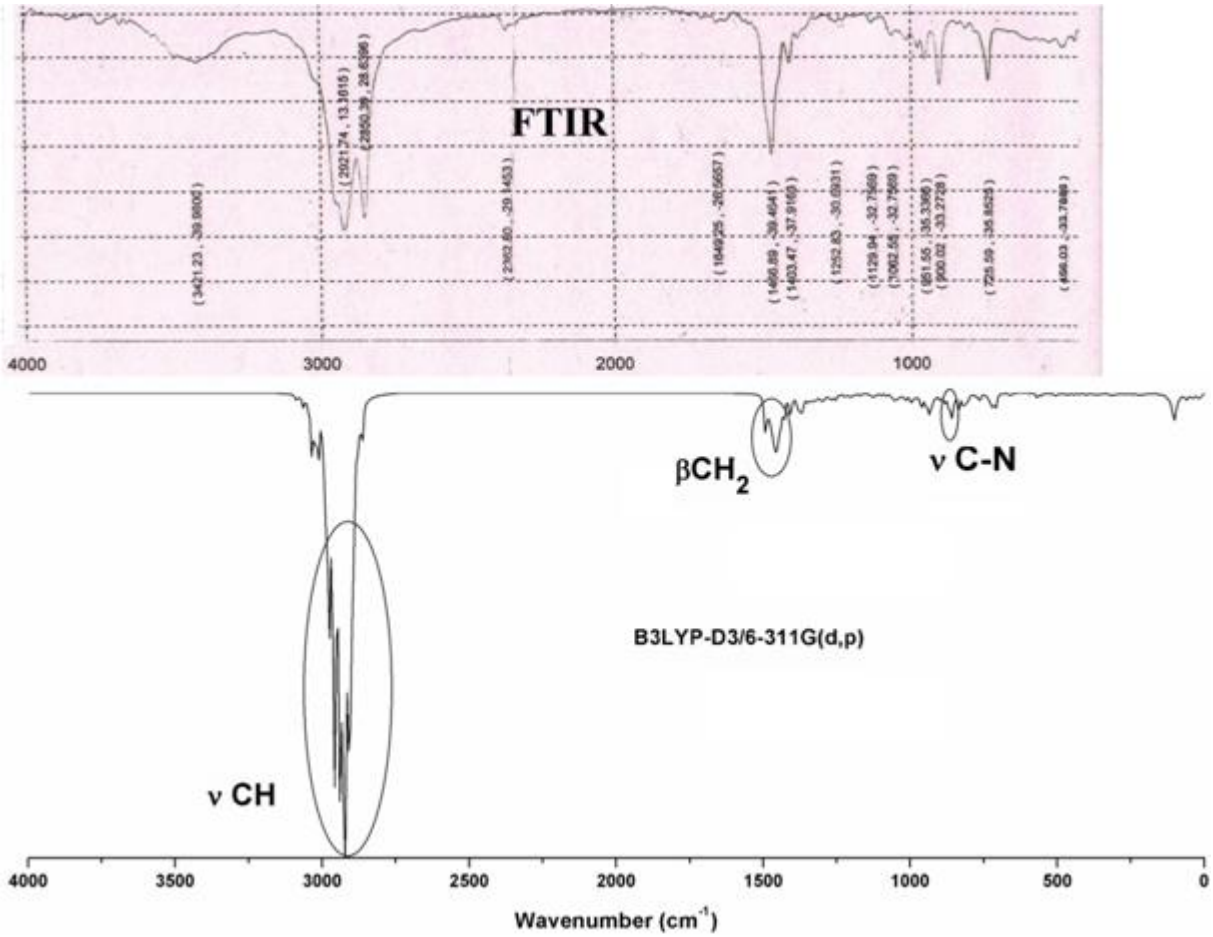

Figure 5S: Comparison of experimental and simulated IR spectra of 16-6-16 [ν: stretching, β: in-plane bending vibrations]